DOI: https://doi.org/10.37434/tpwj2024.03.02

THERMAL CYCLES AND MICROSTRUCTURE OF THE FL ASH BUTT WELDED JOINTS OF 110G13L AND K76F STEEL RAILS THROUGH 08Xh18N10T STEEL INSERT

O.V. Kavunichenko[1], I.V. Ziakhor[1], Yu.A. Shylo[1], A.M. Levchuk[1], Ye.V. Antipin[1], Andrew Fong[2]

[1]E.O. Paton Electric Welding Institute of the NASU
11 Kazymyr Malevych Str., 03150, Kyiv, Ukraine
[2]Yardway Railquip Limited, Unit A5, 29/F., TML Tower, 3 Hoi Shing Road, Tsuen Wan, N.T., Hong Kong

ABSTRACT

The article presents the results of studying the choice of temperature-time and energy-force parameters in flash butt welding (FBW) of the railway crosspiece core (110G13L steel) with rail (K76F steel) through an intermediate chrome-nickel austenitic insert (08Kh18N10T steel). Using an algorithm of numerical solution of the three-dimensional heat conduction equation under the initial and boundary conditions corresponding to the real conditions of welding of the specimens, thermal cycles in FBW of K76F steel with austenitic 08Khl8N10T steel and 110G13L steel with austenitic 08Khl8N10T steel and temperature distribution in welded joints (in the heat-affected zone for both steels) were obtained. Ranges of varying the main technological parameters of the FBW process have been determined, in which during flashing of rails from K76F, 110G13L and 08Khl8N10T steels, their uniform heating across the cross-section and length is provided, sufficient for achieving deformation to the specified extent during upsetting.

KEYWORDS: flash butt welding, railway crosses, rail steel, pulsating flashing

INTRODUCTION

The development of various welding methods made it possible to solve many problems typical for manufacturing products from metal materials. One cannot imagine modern mechanical engineering without welding technologies and other processes accompanied by materials fusion. One of the most difficult problems is related to the formation of permanent combined structures, the elements of which are made of materials with different composition [1].

There are products of critical purpose that determine the safety of railway transport. One of the most typical examples in this field is welded crosses, in the formation of which three types of steels are used [2–4].

The method of producing permanent joints, based on using the technology of flash butt welding of crosses from 110G13L steel with railway rails, largely eliminates the drawbacks characteristic of detachable structures. This technology is used by European and Ukrainian manufacturers of switches. The technological process consists in successive welding of elements from high-manganese and chrome-nickel steels, and then rail steel. Without using intermediate inserts from 08Kh18N10T steel, the quality of joining 110G13L steel and rail steel, which differ sharply in chemical composition and belong to different structural classes, does not meet the operating conditions of switches.

Replacing open-hearth steel with converter steel requires the improvement in the technology for flash butt welding (FBW) of the railway crosspiece core from 110G13L steel with rail ends of K76F steel. In Ukraine, railway rails from oxygen-converter steel — non-heat-strengthened (R260), surface-hardened (R350NT) and surface-hardened, additionally microalloyed with transition metals, in particular vanadium (K76F) and titanium (K76T) are used.

At present, one of the most important parts of the track upper structure used in the railway industry, are crosses. High-manganese austenitic 110G13L steel is successfully used in mechanical engineering. Due to the ability of the operating surface to cold working, 110G13L steel even now is practically irreplaceable for manufacturing products operating under the influence of shock, shock-abrasive loads and high specific static pressures, as for example, tractor caterpillar tracks, rail frogs, switches. Along with its unique properties, the steel has a fairly low cost, so its use has undeniable advantages.

High-manganese 110G13L steel contains 11–13 % Mn and is unique for the reason that it combines high toughness and ductility with a high ability to hardening. Wear resistance depends on the level of intensity of surface hardening and the hardening process during operation [5–8]. Railway rails are made of pearlitic steel, which contains 0.72–0.82% of carbon, up to 1.5 % of manganese and up to 0.5 % of silicon. The physical properties of these two materials create a problem during

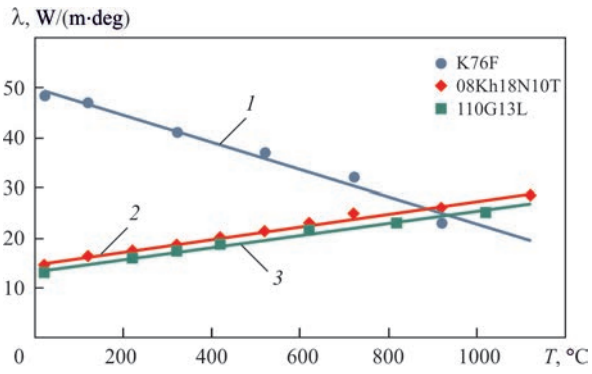

Figure 1. Dependence of coefficient of heat conductivity of welded steels on temperature: *1* — linear (K76F); *2* — linear (08Kh18N10T); *3* — linear (110G13L)

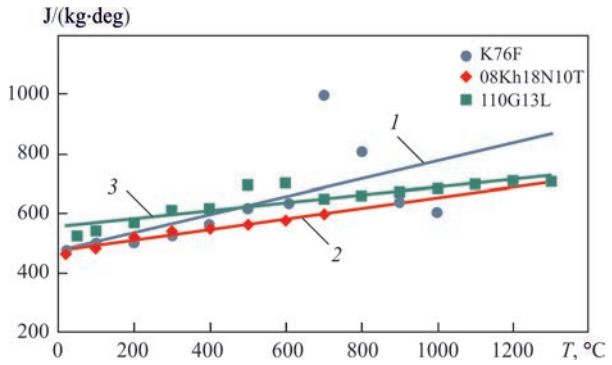

Figure 2. Dependence of specific heat capacity of welded steels on temperature: *1* — linear (K76F); *2* — linear (08Kh18N10T); *3* — linear (110G13L)

Table 1. Mechanical properties of studied steels

Steel grade	σ_t, MPa	σ_y, MPa	δ, %	ψ, %	Hardness, HV_{30}
K76F	485–575	1311–1368	13.5	31	370–380
110G13L	400	800	25	35	205–230
08Kh18N10T	205	510	43	45	140–150

Notes. σ_y — yield strength; σ_t — tensile strength; δ — relative elongation after rupture; ψ — reduction in area after rupture.

welding due to different thermophysical (Figures 1, 2) and mechanical properties (Table 1) [9].

The aim of the work is to establish the influence of temperature-time and energy-force parameters in flash butt welding (FBW) on the formation of structure and phase composition, mechanical characteristics of solid-phase joints of wear-resistant high-manganese 110G13L steel with rail steels through an austenitic chrome-nickel steel insert.

MATERIALS, RESEARCH PROCEDURES AND EQUIPMENT

For research, steels were used, the chemical composition of which is given in Table 2.

Welding was carried out in the K924M machine designed at the PWI. The machine is designed for flash butt welding of railway crosspiece elements from special steel with corresponding parts from rail steel in stationary conditions or for welding rails of 140–195 mm height, with a cross-sectional area from 5000 to 15000 mm^2 with flash removal immediately after welding. The produced welded joints were used to make sections to study their structural features. The strength and ductility of welded butts, elements of railroad crosspieces, were determined by static 3-point bending in the MSP-300 hydraulic press. To evaluate structural features of welded joints, the methods of light (Neophot-32), scanning electron microscopy (JAMP-9500F Auger-microprobe, JEOL with an installed OXFORD EDS INCA Energy 350 spectrometer) were used. The hardness of metal in the HAZ of the welded joint was measured by Vickers in a stationary hardness tester NOVOTEST TS-BRV at a load of P = 300 N.

Prediction of the phase state kinetics of the metal of the joint zone of K76F + 08Kh18N10T and 08Kh18N10T + 110G13L steels in the process of welding and cooling of the welded rail butt was performed on the basis of numerical analysis of temperature cycles under the specific modes of thermal effect, chemical composition of ingot steels and anisotropic austenite decomposition (AAD) diagrams. Such diagrams, taking into account the duration of holding above the corresponding temperatures (austenite grain size number), have now been developed for many steels. With the help of AAD diagrams, it is possible to evaluate the mass fraction Vn of a particular nth structural component (n = A, F, P, B, M, respectively, austenitic, ferritic, pearlitic, bainitic, martensitic) in the areas of both pure as well as mixed phases: austenitic (A), austenitic-ferritic (A + F), pearlitic (A + F + C), where C is carbides adjacent to the zone limited by the temperature of the beginning of martensitic transformation and above by temperatures be-

Table 2. Chemical composition of studied steels

Steel grade	Mass fraction of chemical elements, %							
	C	Cr	Ni	Ti	Mn	Si	S	P
K76F	0.8	–	–	–	1.3	0.35	0.004	0.035
110G13L	1.2	1	1	–	14.5	0.8	0.05	0.12
08Kh18N10T	0.07	17.2	11.8	0.4	1.82	0.6	0.001	0.025

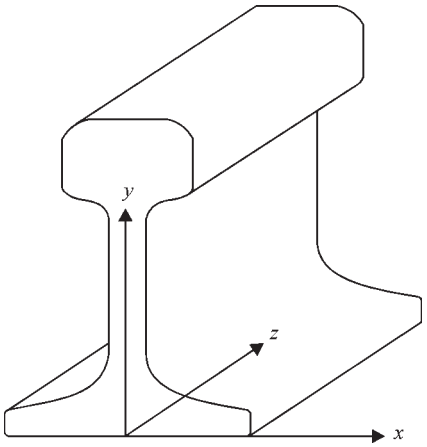

Figure 3. Product to be welded in a rectangular coordinate system

low 600 °C. Accordingly, the points of intersection of the temperature cycle curves $T(t)$, characterized by an average cooling rate in the zone of 800–500 °C determine the temperature of the beginning and end of the corresponding structural transformations of austenite into the n-th phase.

RESEARCH RESULTS AND DISCUSSION

To study the thermal cycles occurring during FBW, a mathematical model of continuous rail heating was developed in cooperation with the Department No. 34 "Mathematical methods for studying physical and chemical processes in welding and special electrometallurgy" of the PWI.

The kinetics of the thermal field in welded rails was described by the equation (1) of heat conductivity with variable thermokinetic characteristics of the material in a three-dimensional coordinate system, shown in Figure 3 [10–12].

$$C\rho(x,y,z,T)\cdot\frac{\partial T(x,y,z)}{\partial t}= \\ =\frac{\partial T(x,y,z)}{\partial x}\cdot\left[\lambda(x,y,z)\cdot\frac{\partial T(x,y,z)}{\partial x}\right]+ \\ +\frac{\partial T(x,y,z)}{\partial y}\cdot\left[\lambda(x,y,z)\cdot\frac{\partial T(x,y,z)}{\partial y}\right]+ \\ +\frac{\partial T(x,y,z)}{\partial z}\cdot\left[\lambda(x,y,z)\cdot\frac{\partial T(x,y,z)}{\partial z}\right]. \quad (1)$$

Taking into account different mechanisms of heat dissipation (convective, infrared radiation), the boundary conditions were described.

$$-\lambda(T)\frac{\partial T(t)}{\partial n}=\alpha(T-T_C)+\varepsilon\cdot\sigma\cdot\left(T^4-T_C^4\right). \quad (2)$$

The heat source in FBW is thermal energy, described by setting boundary conditions in the following form (3), where η is the efficiency coefficient, which takes into account active and reactive losses due to the characteristics of the secondary circuit of the machine; I is the welding current; U is the welding voltage.

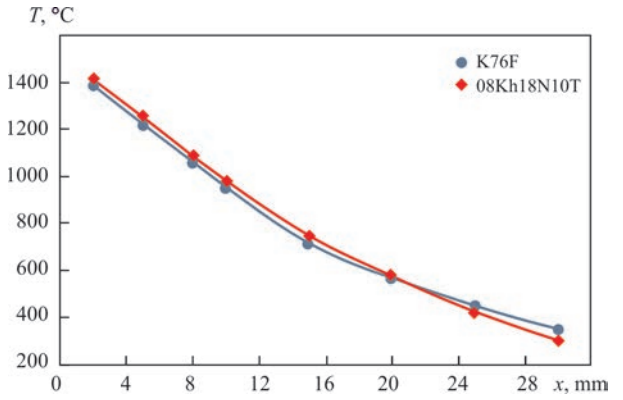

Figure 4. Temperature distribution along the axis of the rails before upsetting at FBW of K76F and 08Kh18N10T steels (calculation)

$$\lambda(T)\frac{\partial T(t)}{\partial n}\bigg|_{z=0}=0{,}5\cdot\eta\cdot U\cdot I. \quad (3)$$

Using a mathematical model of three-dimensional tracing of temperature fields, the temperature distribution over the thickness of the welded joint before upsetting in FBW of K76F with 08Kh18N10T steel was obtained (Figure 4).

To obtain the necessary thermal cycles, the PWI developed a welding technology called pulsating flashing.

Due to the multifactor control of the spark gap between the contacting parts during the flashing process, as well as instantaneous voltage values, intensification of contact heating is ensured, which reduces metal losses during flashing and improves the efficiency coefficient compared to conventional processes of continuous flashing or resistance preheating. The heating period and flashing tolerances are reduced by 1.5 to 2.0 times. High-quality joints are produced with a smaller HAZ width.

The use of pulsating flashing (PF) makes it possible to provide the necessary heating of the rail and austenitic steels, which differ significantly in their thermal properties [13].

Experimental studies of thermal cycles were carried out according to the following scheme. Thermocouples were welded to the rail head at a distance of 5 mm from

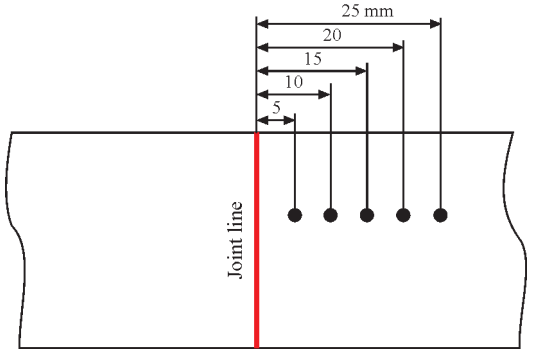

Figure 5. Layout of thermocouples

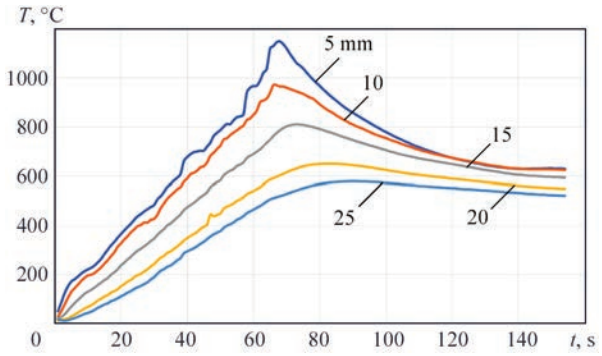

Figure 6. Thermal cycles of FBW at different distance from the joint line of K76F and 08Kh18N10T steels

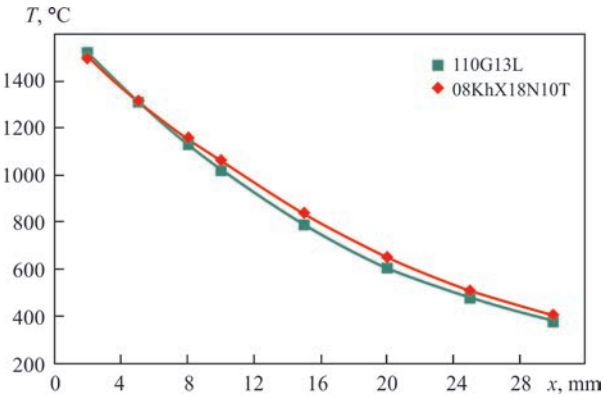

Figure 7. Temperature distribution along the axis of the rails before upsetting at FBW of 08Kh18N10T and 110G13L steels (calculation)

each other (Figure 5). The distance to the first thermocouple was calculated in such a way that after a complete welding cycle, it was 5 mm from the joint line.

The calculated results of thermal cycles coincide with the experimental studies with a small error (Figure 6).

Using a similar procedure, the temperature distribution over the thickness of the welded joint before upsetting in FBW of 08Kh18N10T steel with 110G13L steel was determined by calculation (Figure 7).

In FBW of austenitic (08Kh18N10T + 110G13L) steels, it is necessary to combine more intensive heating with the depth of metal heating. During the experiments, the heating duration at its different intensity, tolerances for flashing and upsetting were varied.

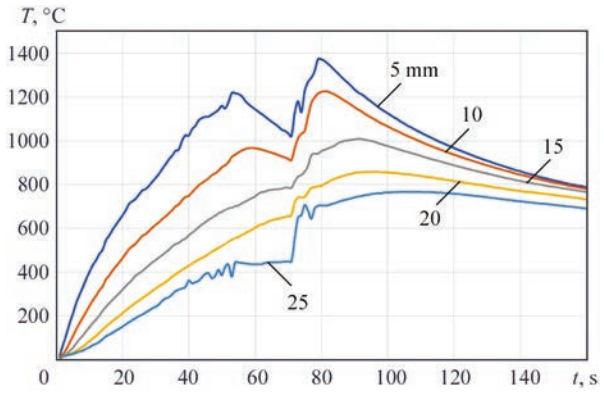

Figure 8. Thermal cycles of FBW at different distance from the joint line of 08Kh18N10T and 110G13L steels

Table 3. Mode for FBW of K76F rail steel with 08Kh18N10T steel

Welding parameters	
Welding tolerance S, mm	30
Voltage U_1, V	280–380
Upsetting, mm	12
End flashing rate V_f, mm/s	1.6–1.8

Table 4. Mode for FBW of 08Kh18N10T with 110G13L steel

Welding parameters	
Welding tolerance S, mm	30
Voltage U_1, V	255–380
Upsetting, mm	13
End flashing rate V_f, mm/s	1.8–2.0

When using the combined heating method (mode), experimental thermal cycles were obtained, shown in Figure 8.

Reducing the voltage at a certain stage of the welding process made it possible to ensure the heating of steels necessary for the thermo-deformation process.

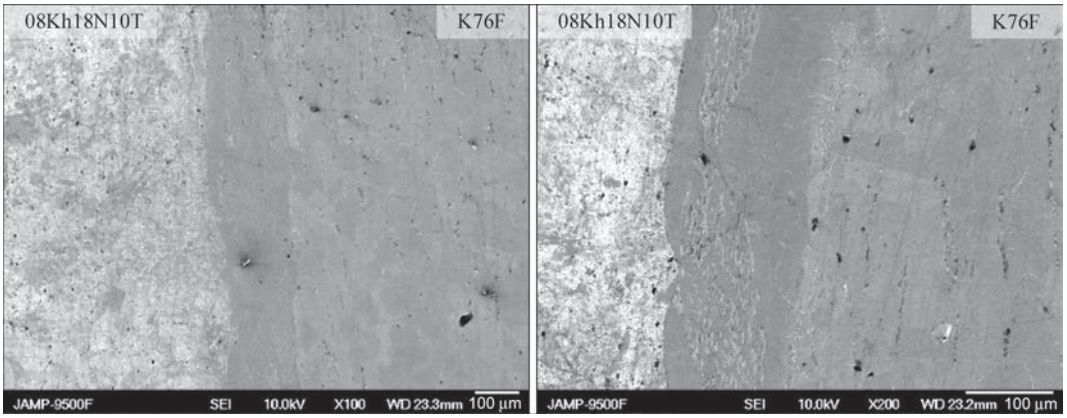

Figure 9. SEM-image of metal microstructure in the transition zone of the joint K76F + 08Kh18N10T steels

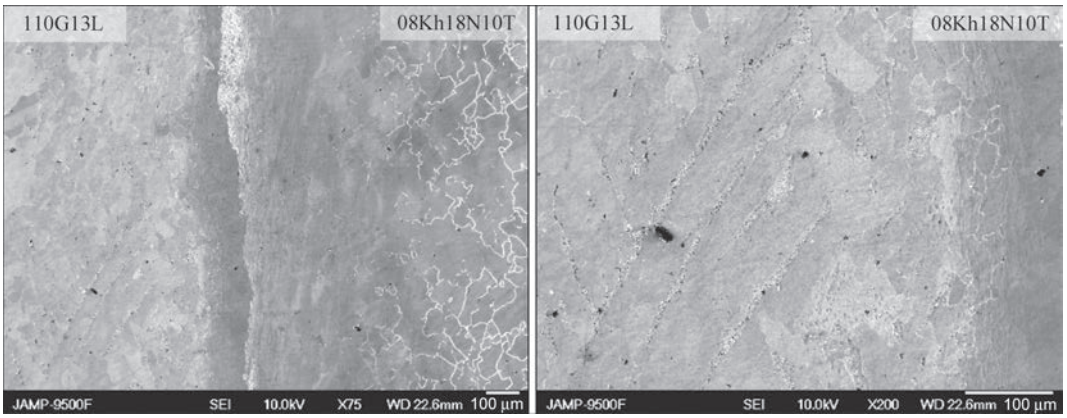

Figure 10. SEM-image of metal microstructure in the transition zone of the joint 110G13L + 08Kh18N10T steels

In the course of the experiments, the duration of heating at different intensities, tolerances for flashing and upsetting values were varied. To ensure the required energy input, a welding mode for K76F rail steel with 08Kh18N10T (Table 3) and 08Kh18N10T with 110G13L steel (Table 4) was selected.

Changing the primary voltage in the range of U_1 = 255–380 V and the displacement velocity V_d = 0.8–2.4 mm/s in the FBW process ensures equalization of temperature gradients in austenitic and pearlitic steels, which allows optimizing the deformation conditions of both steels during the upsetting process and ensuring that the mechanical properties of joints meet regulatory requirements.

The transition zone of the joint K76F + 08Kh18N10T steel (Figure 9) is formed as a result of fusion of subgrain boundaries of the rail steel and heterodiffusion processes. The microstructure of the transition zone is characterized by regions with an acicular structure against a light field. The flashed areas formed in the transition zone correspond to the chemical composition of low-alloy steels. Depending on the cooling rate, the products of the eutectoid austenite transformation in such steels can be pearlite, bainite, or martensite.

The transition zone of the joint 110G13L + 08Kh18N10T steel (Figure 10) has a stable austenitic structure. The joint area with a variable concentration of chemical elements has a width of about 200 µm. At the same time, the transition zone with an almost constant concentration of alloying elements Cr, Mn, and Ni has a width of about 50 µm, which indicates that the welded joint in this zone was formed in a liquid state. The width of diffusion zones in the joint is up to 50 µm in the direction of 08Kh18N10T steel and up to 100 µm in the direction of 110G13L steel (Figure 11).

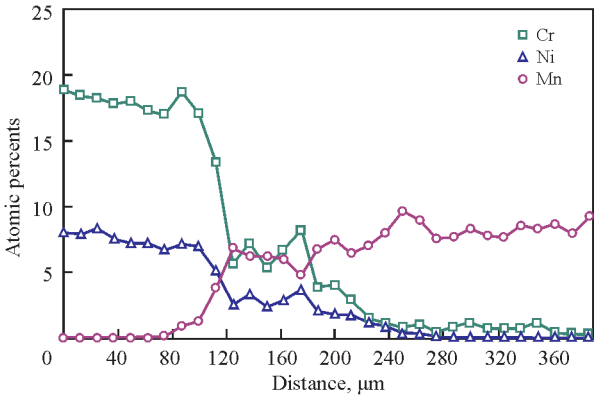

Figure 11. Distribution of chemical elements concentration in the transition zone of the joint 110G13L + 08Kh18N10T steels (at.%)

CONCLUSIONS

1. The influence of temperature-time and energy-force parameters was established and the ranges of changes in the main technological parameters of the FBW process were determined, at which, in the process of flashing rails from K76F, 110G13L and 08Kh18N10T steels, their uniform heating over the cross-section and length is ensured, sufficient to perform deformation at a specified value during upsetting.

2. Using the algorithm for numerical solution of the three-dimensional heat conductivity equation under the initial and boundary conditions corresponding to the actual welding conditions of the specimens, thermal cycles were obtained in FBW of K76F steel with austenitic 08Kh18N10T steel and high-manganese 110G13L with austenitic 08Kh18N10T steel and the temperature distribution in the welded butts (in the heat-affected zone for both steels) was determined.

3. The thermal cycles in FBW of K76F and 110G13L steels with an intermediate insert of 08Kh18N10T steel at different values of the main technological parameters of the welding process were determined, and the influence of the FBW process on structural changes in the zone of joining the 1st and 2nd butts was established.

4. The range of changes in the primary voltage U_1 and the displacement velocity V_d (U_1 = 255–380 V and V_d = 0.8–2.4 mm/s) in the process of flash butt welding, at which the equalization of temperature gradients in austenitic and pearlite steels is provided,

which allows optimizing the deformation conditions of both steels in the process of upsetting and ensuring the compliance of mechanical properties of the joint with regulatory requirements, has been established.

REFERENCES

1. Gotalsky, Yu.N. (1981) *Welding of dissimilar steels*. Kyiv: Tekhnika [in Russian].
2. Kuchuk-Yatsenko, S.I., Kavunichenko, O.V., Ma, Ping et al. (2017) Technology and equipment for flash butt welding of railway frogs with rail ends through austenitic insert. *Railway Eng. China*, **12**, 102–105.
3. Kuchuk-Yatsenko, S.I., Shvets, Yu.V., Kavunichenko, O.V. et al. (2015) Flash butt welding of railway frogs through cast austenitic insert. *The Paton Welding J.*, **8**, 5–7. DOI: https://doi.org/10.15407/tpwj2015.08.01
4. Kavunichenko O.V., Shvets V.I. and Antipin E.V. (2018) Peculiarities of flash-butt welding of rail frogs with rail ends. *The Paton Welding J.*, **4**, 19–24. DOI: https://doi.org/10.15407/tpwj2018.04.04
5. Karaman, I., Sehitoglu, H., Chumlyakov, Y. et al. (2001) Extrinsic stacking faults and twinning in Hadfield manganese steel single crystals. *Scripta Mater.*, **44**, 337–443.
6. Efstathiou, C. (2009) Strengthening Hadfield steel welds by nitrogen alloying. *Materials Sci. and Eng.*, **506**, 174–179.
7. Efstathiou C., Sehitoglu H. (2010) Strain hardening and heterogeneous deformation during twinning in Hadfield steel. *Acta Materialia*, **58**, 1479–1488.
8. Mohyla, P. (2004) Affect of tempering temperatures on mechanical properties of weld joints in low-alloyed creep-resistant steels. *Acta Metallurgica Slovaca*, **10**, 193–200.
9. (2003) *Grades of steels and alloys*: Refer. Book. Ed. by A.S. Zubchenko. Mockow, Mashinostroenie.
10. Olivares, R., Garcia, C., DeArdo, A. et al. (2011) Advanced metallurgical alloy design and thermo mechanical processing for rails sleels for North American heavy use. *Wear*, **271**, 364–373.
11. Sahay, S., Mohapatra, G., Totten, G. (2009) Overview of Pearlitic Rail Steel: accelerated cooling, quenching, microstructure, and mechanical properties. *J. ASTM Int.*, **7**, 1–26.
12. Alves, L., Lagares, M., Filho, R. et al. (2019) Predictive mathematical modeling of the flash-butt welding process to optimize the properties of welds of premium and super premium rails. In: *Proc. of Inter. Heavy Haul STS Conf., 10–14 June, Narvik, Norway, 2019*.
13. Kuchuk-Yatsenko, S.I. et al. (2001) *Method of flash-butt welding*. Pat. US6294752B1. 219.100.

ORCID

O.V. Kavunichenko: 0000-0002-5164-9796,
I.V. Ziakhor: 0000-0001-7780-0688,
Yu.A. Shylo: 0000-0002-6174-5925,
A.M. Levchuk: 0000-0002-0361-7394,
Ye.V. Antipin: 0000-0003-3297-5382,
Andrew Fong: 0009-0000-3996-4403

CONFLICT OF INTEREST

The Authors declare no conflict of interest

CORRESPONDING AUTHOR

O.V. Kavunichenko
E.O. Paton Electric Welding Institute of the NASU
11 Kazymyr Malevych Str., 03150, Kyiv, Ukraine.
E-mail: avkava@gmail.com

SUGGESTED CITATION

O.V. Kavunichenko, I.V. Ziakhor, Yu.A. Shylo, A.M. Levchuk, Ye.V. Antipin, Andrew Fong (2024) Thermal cycles and microstructure of the flash butt welded joints of 110G13L and K76F steel rails through 08Xh18N10T steel insert. *The Paton Welding J.*, **3**, 9–14.

JOURNAL HOME PAGE

https://patonpublishinghouse.com/eng/journals/tpwj

Received: 17.10.2023
Received in revised form: 05.12.2023
Accepted: 04.04.2024